

A SPECTRAL DATABASE OF CALCIUM-ALUMINUM-RICH INCLUSIONS AND APPLICATIONS TO ASTEROID OBSERVATIONS. J. M. Mueller¹, B. L. Ehlmann¹, G. R. Rossman¹, R. N. Greenberger¹, R. T. Marquez¹, M. A. Ivanova², F. L. H. Tissot¹, K. de Kleer¹, ¹Division of Geological & Planetary Sciences, California Institute of Technology, Pasadena, CA 91125, USA (jmmuelle@caltech.edu), ²Vernadsky Institute, Kosygin St. 19, Moscow 119991, Russia

Introduction: As the oldest known Solar System (SS) solids [1], Calcium-aluminum-rich inclusions (CAIs) are key to constraining the age and initial isotopic composition of the SS, as well as the mineralogical compositions of the first phases condensed out of the solar nebula [2]. From the few studies that have investigated the infrared reflectance properties of CAIs [4-8], they are associated with a near-infrared (NIR) broad 2- μm absorption and an absent 1- μm absorption (which would indicate Fe-bearing pyroxene and/or olivine) [4,5] as well as mid-infrared (MIR) features at 11.7, 12.4, 14.1, and 14.3 μm [8]. The NIR signature is characteristic of spinel [9], a key phase in CAIs [2]. As such, spinel-like reflectance in telescopic data has been used to estimate CAI abundances in asteroids. Although CAI abundances in the meteorite collection are <4% [10], unique spectroscopic and polarimetric characteristics of L-type asteroids have led to the hypothesis that they might contain up to 30% of CAIs [11,12].

If true, this could indicate that L-type asteroids are among the most ancient asteroids in the SS. However, asteroids with such high CAI content should have melted and homogenized in the presence of the short-lived radioisotope ²⁶Al. A CAI-enriched asteroid formed in the absence of this early SS heat source [3], would reshape our understanding of early SS processes.

We performed laboratory work to create a robust framework for characterizing NIR and MIR CAI reflectance spectra that will be used to interpret infrared observations of L-type asteroids from the James Webb Space Telescope's (JWST) first observing cycle. NIR and MIR spectra of these asteroids will together confirm or refute the 30% CAI abundance hypothesis and will shed light on the origin of these unusual objects.

Methods: Sample Selection. A diverse group of 20 CAI samples were obtained from Caltech's Isopotarium (Fig. 1). The diversity of CAIs is based on petrologic and textural type. The initial selection included 9 fine-grained (fg) CAIs (spinel and Ca-pyroxene dominated) and 11 coarse-grained (cg) CAIs. Within the cg-samples, 4 type A (melilite dominated), 4 type B (spinel and Ca-pyroxene dominated), and 3 ungrouped CAIs were selected. Sample triage removed altered samples (Fig. 1).

Data Acquisition. Microimaging NIR reflectance spectra were acquired using the Ehlmann lab's imaging spectrometer comprised of a visible/near-infrared

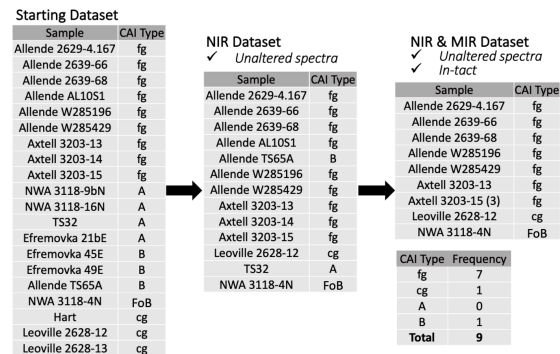


Fig. 1. CAI dataset evolution: from initial collection (n=20), to NIR (n=13), and MIR screened dataset (n=9). FoB indicates forsterite-rich Type B CAI.

(VNIR) sensor (0.4-1 μm region; $\sim 71 \mu\text{m}/\text{pixel}$) and a shortwave infrared sensor (SWIR) sensor (0.9-2.6 μm ; $\sim 212 \mu\text{m}/\text{pixel}$). MIR reflectance measurements from 2.5-14 μm with a resolution of 4 cm^{-1} and 60 $\mu\text{m}/\text{spot}$ were obtained in the Rossman lab using a micro-FTIR and CsI beam splitter. For each CAI, the number of spectra collected varied based on the size/condition of the sample. The location of each spectrum on the CAI was not tracked in detail for this preliminary study, but will be in future work.

Spectral analysis. Infrared spectra were analyzed using the Workbench for Imaging Spectroscopy Exploration and Research (WISER) software [13]. NIR spatial heterogeneity was evaluated for each sample (Fig. 2). Band depth maps of water (1.9 μm) and spinel (2 μm) were used to characterize the spatial distribution of alteration and the primary mineral of interest (Fig 3).

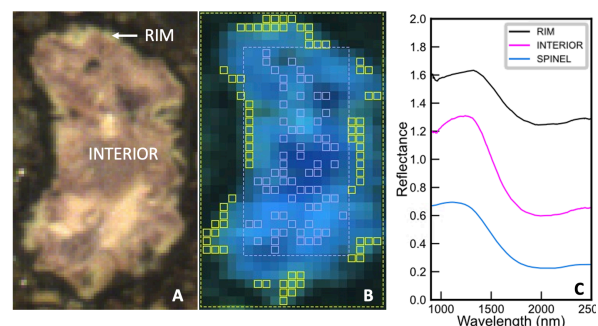


Fig. 2. (A) VNIR image and (B) SWIR image of Allende 2629-4.167 CAI overlaid with multi-pixel selection regions of interest (yellow & purple boxes). (C) Spectral heterogeneity could stem from the rim/interior mineralogical variability of the sample. However, our samples showed minimal to no spectral variation and were comparable to library reference spinel in the VNIR.

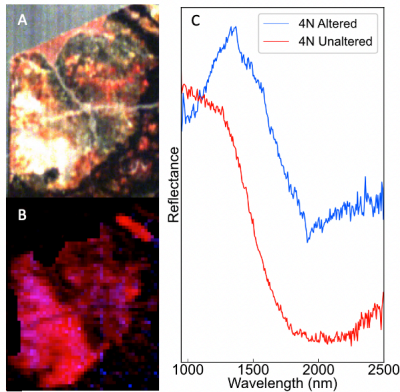


Fig. 3. (A) VNIR image of NWA 3118 4N. (B) SWIR RGB band map showing the spinel-associated 2 μm absorption (red) and the 1.9 μm water absorptions (blue). Brighter pixels correspond to deeper absorptions. (C) Altered and unaltered spectra from 4N. In this sample, water and spinel associated absorptions are often coincident, though the 2 μm absorption is fairly ubiquitous.

Library reference spectra for comparison to sample spectra were sourced from RELAB, ECOSTRESS, and CRISM spectral databases.

Preliminary Results: Near-infrared. Early in the near-infrared analysis of our starting dataset, significant to moderate water alteration at 1.9 μm was observed in all cg-CAIs, while fg-CAIs did not show such alteration. An absorption at 1.9 μm can indicate terrestrial alteration, which led us to remove altered samples (Fig. 1), and examination of 1.9 μm band maps (Fig. 3) allowed us to extract water-free pixels from 2 cg-CAIs and retain them in the final dataset, along with 7 fg-CAIs.

The NIR spectra of the 9 CAIs in the final dataset were compared to library references and to each other (Fig 4). Absorptions at 0.55 μm , 0.6, and 2 μm were observed. The origin of the 0.55 μm and 0.6 μm absorptions could be Fe intervalence charge transfer (IVCT) or Cr IVCT (specifically related to spinel). The broad, deep 2 μm absorption likely originates from the spinel content of the samples [4,5]. Due to the location of the VNIR and SWIR join near 1 μm , it is difficult to ascertain if this absorption is present or an artifact, and additional spectral data are being acquired.

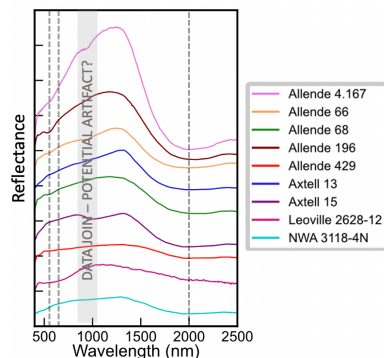


Fig. 4. NIR results for final dataset. Spectra are averages from water-free pixels. The 2 μm absorption is strong in 6 cg, weak in 1 fg and 1 cg, and is curiously absent in 1 cg. A narrow 0.55 μm absorption occurred in 1 fg and 1 cg, while a broad 0.6 μm absorption occurred in 1 cg CAI.

Mid-infrared. Initial analysis of our MIR data revealed an unexpected level of heterogeneity. Though there is some intrasample homogeneity, intersample comparison has revealed that no two MIR signatures of CAIs in our dataset are the same (Fig 5). This is unexpected due to the large number of fg-CAIs in our final dataset, which one may expect to be fairly homogeneous, especially considering their homogeneity in the NIR. Additionally, the MIR signatures exhibit spectral signatures characteristic of olivine and pyroxene whereas the NIR data that lack evidence of these phases preclude more than 10-15 wt% being present.

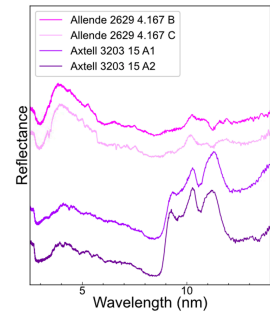


Fig. 5. Duplicate spectra from the same CAI reveal (i) intrasample homogeneity, and (ii) intersample heterogeneity, from the shape and depth of the Christiansen Feature to the varied shapes and positions of the silicate fundamental features.

Conclusions and Future Work: We obtained in-situ hyperspectral NIR data for 20 CAIs (13 unaltered) and in-situ MIR data for 9 CAIs. Water alteration was ubiquitous in cg-CAIs. IVCT absorptions at shorter wavelengths and broad 2 μm absorptions in the NIR are consistent with spinel-dominated CAIs, as in previous studies. Future work will acquire spectra of a subset of the CAIs on an instrument without a VNIR-SWIR join to better characterize the 1 μm region. Additionally, we will use grid-mapping to obtain micro-FTIR measurements over the same areas as the NIR data to enhance our understanding of combined VSWIR-MIR spatial variability in spectra of our samples. We will also attempt to reproduce our spectra using mineral mixing models of the primary CAI phases. These data will be utilized to understand infrared observations of L-type asteroids from the JWST.

Acknowledgements: We thank the Field Museum (Chicago), the American Museum of Natural History (New York), and the Museum of Natural History (Smithsonian Institution, Washington DC) for providing samples.

References: [1] Amelin Y. et al. (2002) *Science*, 297, 1678-1683. [2] MacPherson G.J. (2014) *Treatise on Geochemistry*, 139-179. [3] MacPherson G.J. et al. (2005) *Chondrites & the Protoplanetary Disk*, 341, 225-250. [4] Cloutis E.A. & Gaffey M.J. (1993) *Icarus*, 105, 568-579. [5] Rajan S. & Gaffey M.J. (1984) *LPSC XV*, 659-660. [6] Morlok A. et al. (2004) *Chondrites & Protoplanetary Disk*, 8-11 [7] Melwani Daswani M. et al. (2014) *LPSC XLV*, 2436. [8] Morlok A. et al. (2020) *PSS*, 193. [9] Fabian D. et al. (2001) *Astronomy & Astrophysics*, 373, 1125-1138. [10] Hezel D.C., et al. (2008) *MAPS*, 43, 1879-1894. [11] Sunshine, J.M. et al. (2008) *Science*, 320, 514-517. [12] Devogèle M. et al. (2018) *Icarus*, 304, 31-57. [13] Greenberger et al., this conf.